University of Lethbridge

Atomic-Level Characterization of the Structural Dynamics of Proteins

Shaw et al., 2010

Presented by Jenna Sullivan

April 17, 2023

FiP35

BPTI

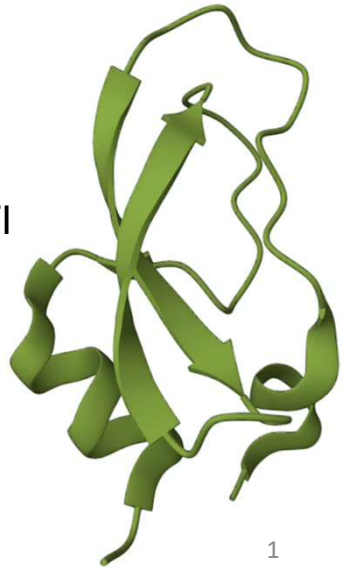

Presentation Outline

- Background
  - Protein folding
  - WW domains (FiP35) and BPTI
- Methods & Results
- Summary/conclusion

Protein Folding and Conformational Changes

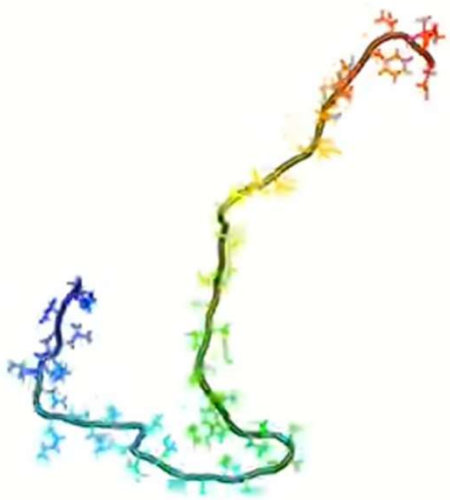

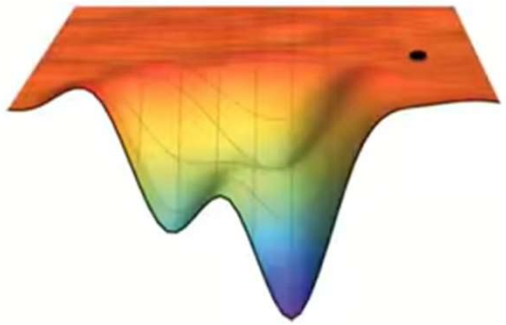

- Protein folding = essential for protein function
- Intramolecular motion of proteins is also important for functionality

(C. Fennell, Junior Fellow, Laufer Center for Physical and Quantitative Biology, Stony Brook University)

WW domains

- Three β strands in a double-hairpin motif
- Model system used in studying the folding and unfolding of beta-hairpins

FiP35 – variant of the human Pin1 WW domain

(Jonsson et al., 2012)

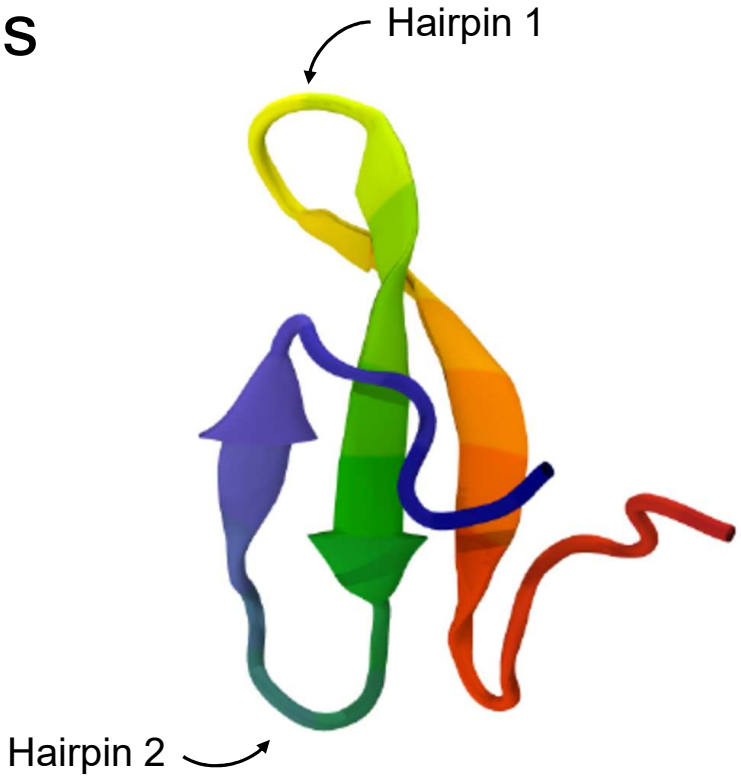

Figure 1. Cartoon representation of FiP35 protein, where red is N terminus and blue is C terminus (Covino et al., 2013).

Bovine pancreatic trypsin inhibitor (BPTI)

- The subject of the first nuclear magnetic resonance (NMR) experiments of internal motion of proteins.

- **Intramolecular motion**: several water molecules exchange, aromatic rings rotate, and a disulfide bridge isomerizes.

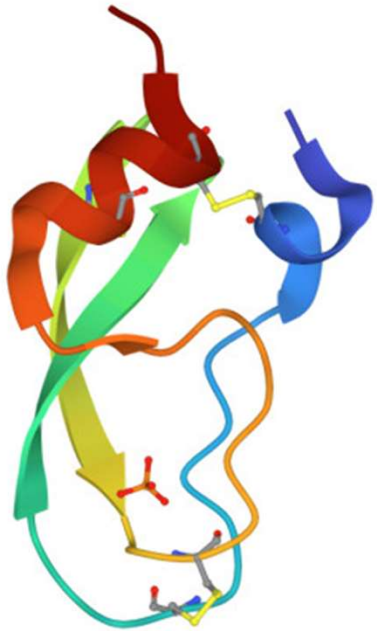

Figure 2. PDB X-ray diffraction structure of BPTI (PDB ID: 5PTI)

All-Atom Molecular Dynamics (MD) Simulations → Used to study the motions of biological macromolecules

Problem?

At the time of the study, computational constraints have limited simulations to ~1 μs, limiting the usefulness of MD

Solution:

Anton: special-purpose supercomputer capable of producing continuous trajectories up to 1 ms in length

Allows more insight into protein folding and different structural states in folded protein

Study Goals

- Describe the folding of the FiP35 WW domain
- Describe the folded-state dynamics of BPTI

Methods for FiP35

Computational Set Up and Simulation Protocols:

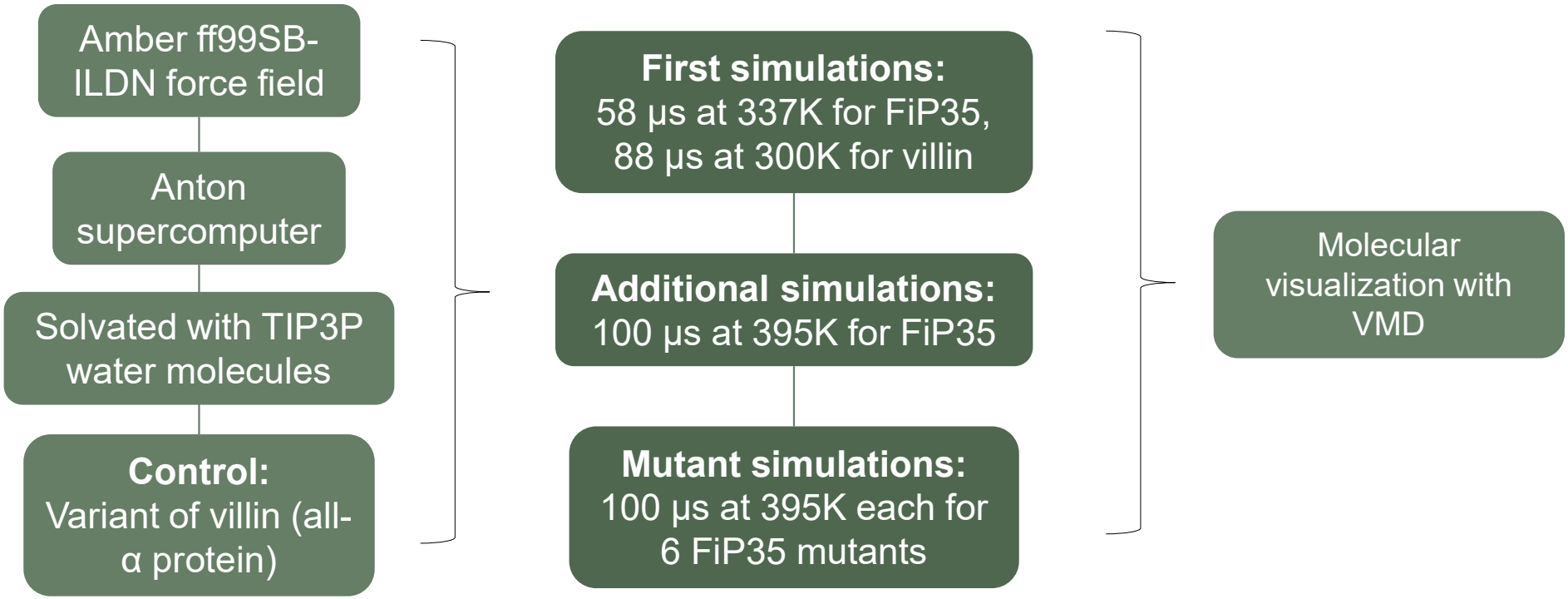

FiP35 Results (1)

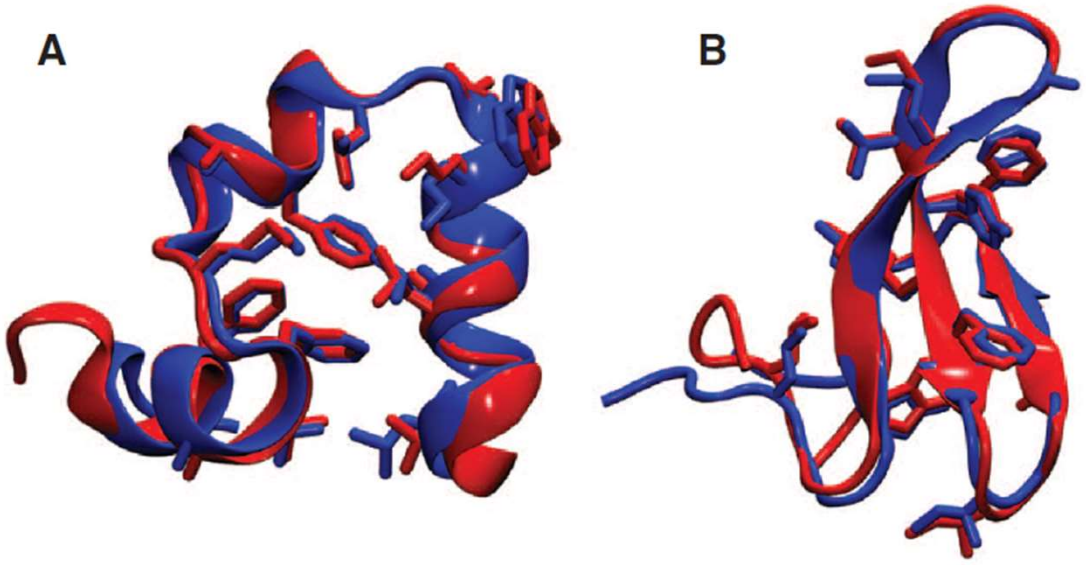

- FiP35 stably folded to a conformation with a backbone **root-mean-squared deviation** (RMSD) of ~1 Å from the crystal structure
- Villin also folded to an RMSD of ~1 Å

Figure 3. Folding proteins at x-ray resolution, showing comparison of x-ray structures (blue) and last frame of MD simulation (red). (A) Simulation of villin at 300K, (B) simulation of FiP35 at 337K.

FiP35 Results (2)

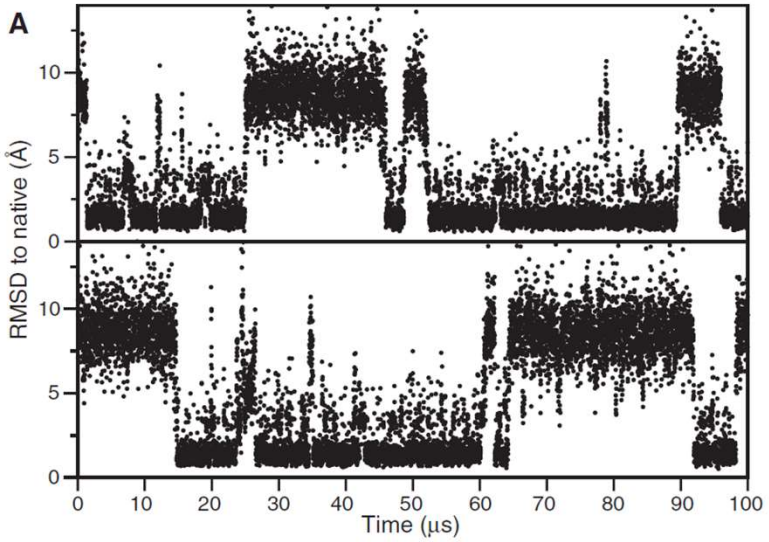

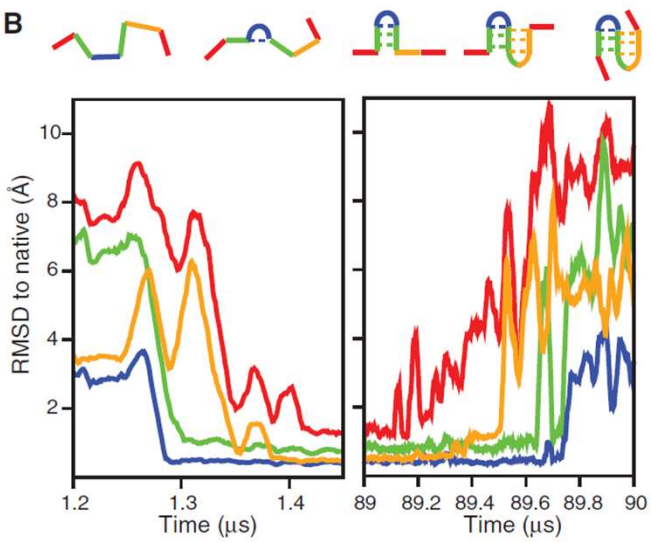

- FiP35 underwent multiple folding and unfolding transitions
- Average folding time = 10 ± 3 μs
- Folding dominated by a single pathway

Figure 4. (A) RMSD time series of two independent 100 μs simulations of FiP35 initiated from an extended state. (B) representative sequence of events leading to folding (left) and unfolding (right).

Methods for FiP35 (2)

Determine the transition state ensemble (TSE):

$$r(x) = \sum_{i=3}^{33} w_i e^{-\frac{1}{2}MSD(i-2,i+2)}$$

where:

r(x) = reaction coordinate

wi = "weights"

MSD = mean square displacement

Assign trajectory frames to the TSE

Commitment probability (P_{fold}) analysis:

4 simulations ran on 101 frames randomly taken from TSE and ran until either:
folded (r(x) < 0.1) or unfolded (r(x) > 0.55) states were reached

P_{fold} = ratio between trajectories that folded and the total number of runs

Methods for FiP35 (3)

φ-value calculation:

$$\varphi_i = \frac{N_i^{TSE} - N_i^U}{N_i^F - N_i^U}$$

Where:

N_i = native side-chain contacts

TSE = transition state

F = folded

U = unfolded

Contact = every time two heavy atoms more than one residue apart were closer than 6 Å

Calculated for every frame of the simulation, assigning each frame to the transition, folded, or unfolded state

Also calculated side-chain φ-values for the six mutants

FiP35 Results (3)

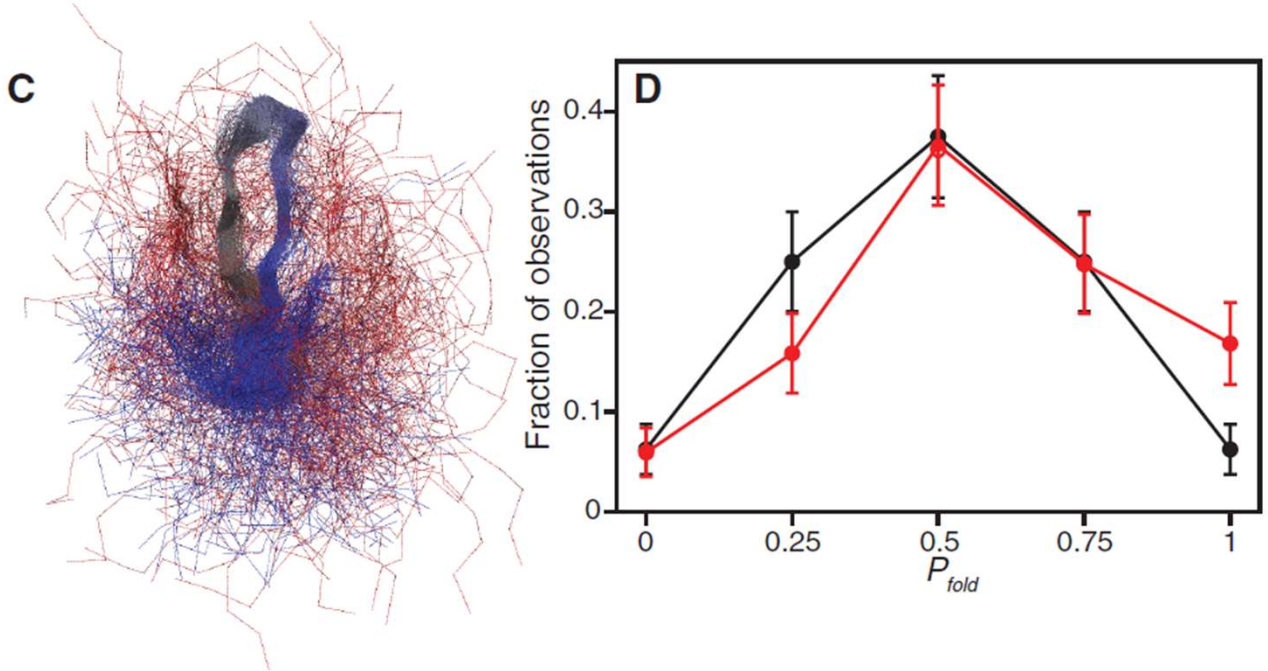

- First hairpin is structured in the transition state for folding
- P_{fold} distribution peaks at 0.5 = resembling ideal TSE
- This verifies the TSE

Figure 5. (C) representative members of the TSE. (D) P_{fold} distribution of the TSE. The observed distribution of Pfold (red) is compared with binomial distribution expected for a true TSE (black).

FiP35 Results (4)

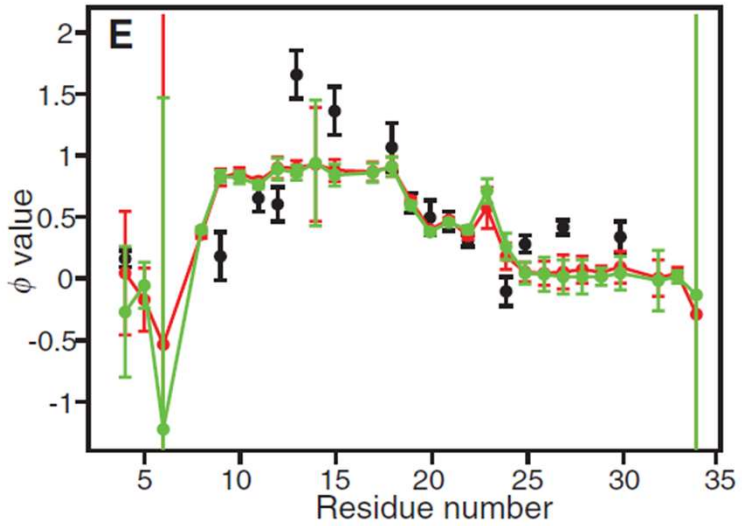

Figure 6. (E) Comparison of experimental and calculated φ values. Two sets of φ values (red and green) calculated from the two simulations and are compared to the experimental values (black) for wild-type Pin1 WW domain.

Table 1. computational φ-value analysis of FiP35.

Mutation	ϕ Value		$\Delta\Delta G_{mut}$ (kcal mol^{-1})	
	MD	Contact approx.	MD (±SEM)	Experiment
Leu^{4} → Ala	−0.6	−0.1	0.5 (0.4)	1.5
Trp^{8} → Phe	−0.1	0.4	1.6 (0.4)	1.8
Arg^{11} → Ala	0.2	0.8	1.8 (0.5)	1.7
Ser^{13} → Ala	1.1	0.9	0.4 (0.5)	n/a
Tyr^{19} → Leu	0.3	0.7	1.1 (0.4)	1.1
Phe^{21} → Leu	0.4	0.5	2.4 (0.5)	1.4

- First hairpin is fully formed in the TSE
- Most of the mutant φ-values were in reasonable agreement with the φ-values calculated from the TSE

Methods for FiP35 (4)

Free energy landscape determination:

Analysed the two 100 μs simulations

Projected the free energy landscape on the optimized reaction coordinate r(x)

T-jump experiment:

Langevin simulations on a model free energy landscape

Langevin equation

$$m\frac{\mathrm{d}v}{\mathrm{d}t} = -\gamma v + R(t)$$

Friction force

Random force

white Gaussian noise

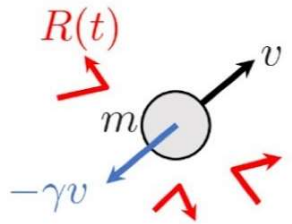

Langevin Equation

FiP35 Results (4)

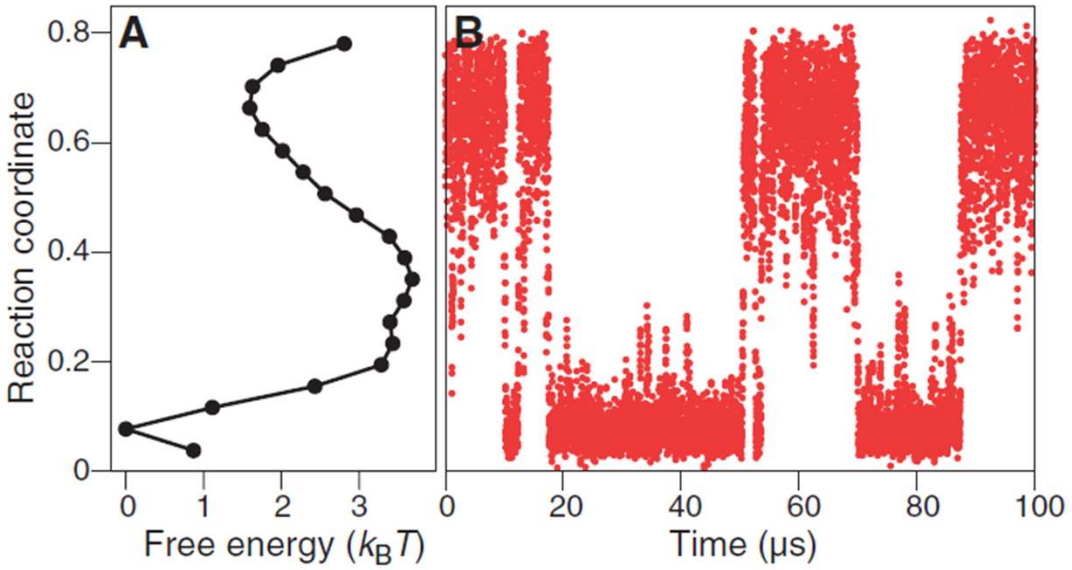

- Transition-state region is broad and flat
- Two local minima
- Observe a slow phase associated with folding, and a fast “molecular” phase

Figure 7. (A) Free-energy profile along an optimized reaction coordinate. (B) Langevin simulation of WW folding in a 1-D model

BPTI Methods

Simulation protocol:

Variant of Amber ff99SB force field

4-particle TIP4P-Ew water model

Anton supercomputer

Simulation: 1 ms at 300K

Fast relaxation analysis

Kinetic clustering scheme:

$$A(x_k, m) = \frac{\sum_{t=1}^{N} \delta_{m,m(t)} x_k(t)}{\sum_{t=1}^{N} \delta_{m,m(t)}}$$

$$\tilde{x}_k(t) = A(x_k, m(t))$$

$$C_{\tilde{x}_k}(\tau) = \left\langle \tilde{x}_k(t) \tilde{x}_k(t+\tau) \right\rangle_t$$

$$E = \sum_{k=1}^{K} \sum_{\tau=\tau_1}^{\tau_2} \left(C_{\tilde{x}_k}(\tau) - C_{x_k}(\tau) \right)^2$$

Dynamical content analysis:

Calculate the time-autocorrelation function

BPTI Results (1)

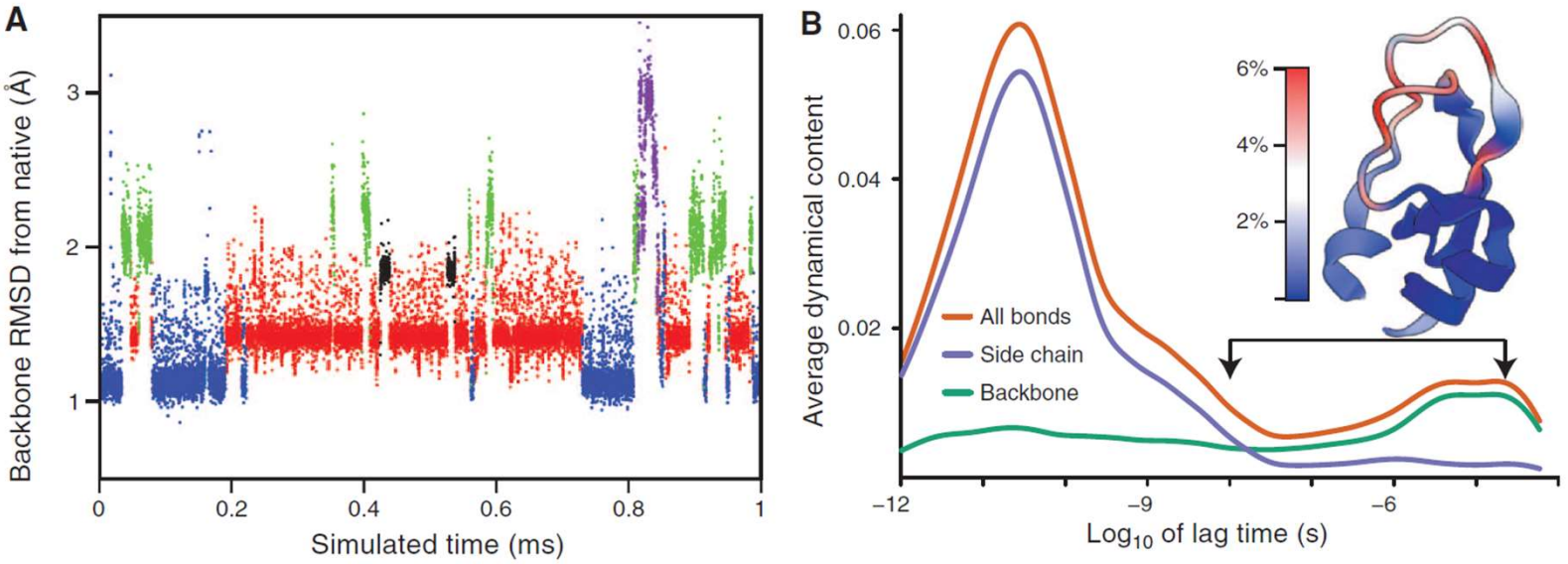

- Two primary conformational states
- Fast relaxations – side-chain motions
- Slow relaxations – backbone motions

Figure 8. (A) All-residue backbone RMSD from the crystal structure with PDB ID 5PTI. (B) Dynamical content its decomposition into side-chain and backbone contributions

BPTI Methods (2)

Analysis of rotating aromatic rings:

Analysis of the χ2 dihedral angles of Tyr and Phe residues

Extract time series of the dihedral angles from the BPTI trajectory

Estimate the probability density functions of the aromatic rings' χ2 angles

Estimation of lifetime distribution of internal waters:

Stable States Picture (SSP) algorithm (Grote & Hynes, 1980)

$$\kappa_f = \int_0^\infty dt \langle j_i(S_R) j_o^*(S_P, t) \rangle_R$$

$$\kappa_f = \langle j_i(S_R) \rangle_R + \int_0^\infty dt \langle j_i(S_R) j_o^*(S_R, t) \rangle_R$$

$$\kappa_f = \int_0^\infty dt \, \langle j_i(S_R) j^*(S, t) \rangle_R$$

BPTI Results (2)

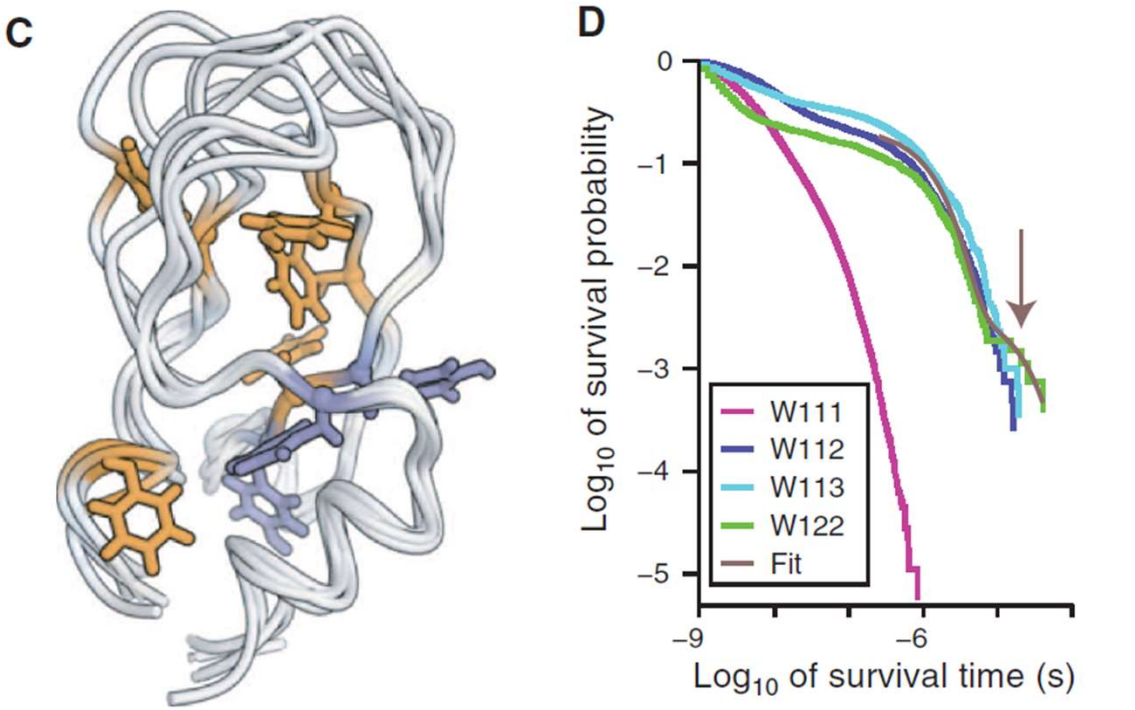

- Seven out of 8 aromatic rings rotated during the simulation
- Three distinct behaviours for four internal water molecules

Figure 9. (C) Crystal structure of BPTI, highlighting the aromatics that rotate slowly in purple and those that rotate quickly in orange. (D) Survival probability distributions for each of the four internal water molecules of BPTI. The arrow at 14 μs mark the lifetime of the slowest waters.

Conclusion/Summary

Anton supercomputer is successful in performing continuous, all-atom MD simulations of proteins

Able to successfully simulate FiP35 protein folding and determining the TSE and the sequence of events for folding.

Were able to successfully simulate BPTI and therefore interpret the folded-state kinetics.

Thank you!

Questions?

References

- Covino, R., Škrbić, T., Beccara, S., Faccioli, P., Micheletti, C. (2013). The Role of Non-Native Interactions in the Folding of Knotted Proteins: Insights from Molecular Dynamics Simulations. *Biomolecules, 4*(1), 1-19. https://doi.org/10.3390/biom4010001
- Grote, R. F., Hynes, J. T. (1980). The Stable States Picture of Chemical Reactions. II. Rate Constants for Condensed and Gas Phase Reactions Models. *J. Chem. Phys.* 73, 2715-2732. https://doi.org/10.1063/1.440485
- Jonsson, A. L., Fersht, A. R., Daggett, V. (2012). 3.1 Combining Simulation and Experiment to Map Protein Folding. *Comprehensive Biophysics*, 1-18. https://doi.org/10.1016/B978-0-12-374920-8.00301-5
- Shaw, D. E., Maragakis, P., Lindorff-Larsen, K., Piana, S., Dror, R. O., Eastwood, M. P., Bank, J. A., Jumper, J. M., Salmon, J. K., Shan, Y., Wriggers, W. (2010). Atomic-level Characterization of the Structural Dynamics of Proteins. *Science*, *330*(6002), 341–346. https://doi.org/10.1126/science.1187409